NANO LETTERS

Letter

pubs.acs.org/NanoLett

Efficient Coupling of an Antenna-Enhanced nanoLED into an Integrated InP Waveguide

Michael S. Eggleston and Ming C. Wu*

Department of Electrical Engineering and Computer Sciences, University of California, Berkeley, California 94720, United States

Supporting Information

ABSTRACT: Increasing power consumption in traditional on-chip metal interconnects has made optical links an attractive alternative. However, such a link is currently missing a fast, efficient, nanoscale light-source. Coupling nanoscale optical emitters to optical antennas has been shown to greatly increase their spontaneous emission rate and efficiency. Such a structure would be an ideal emitter for an on-chip optical link. However, there has never been a demonstration of an antenna-enhanced emitter coupled to a low-loss integrated waveguide. In this Letter we demonstrate an optical antenna-enhanced nanoLED coupled to an integrated InP waveguide. The nanoLEDs are comprised of a nanoridge of InGaAsP coupled to a gold antenna that exhibits a 36× enhanced rate of spontaneous emission. Coupling efficiencies as large as 70% are demonstrated into an integrated waveguide. Directional antennas also demonstrate direction emission down one direction of a waveguide with observed front-to-back ratios as high as 3:1.

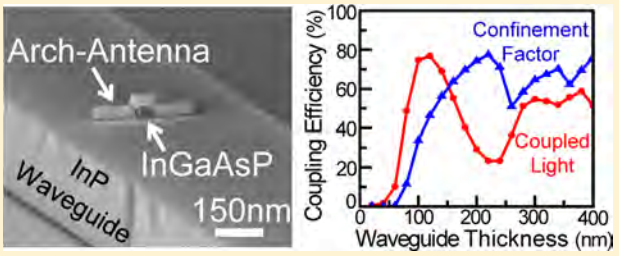

KEYWORDS: *Nanophotonics, optical antennas, enhanced spontaneous emission, integrated waveguide, metal optics, emission coupling*

For decades, lasers have provided the backbone of high-speed long-distance communication. Dramatic advances in semiconductor processing and packaging technology have been able to shrink the laser to smaller sizes, bringing its advantages of high power efficiency and speed to shorter and shorter ranges.[1] On-chip communication is currently an area completely dominated by electrical links that could greatly benefit from optical interconnects; however significant reductions in size and power consumption must be made before optical links can be realized at such a small scale.[2] Metal optics have been able to shrink lasers to the nanoscale,[3−7] but high losses in metal-based cavities have made it exceedingly difficult to achieve efficient lasing at smaller dimensions.[8]

Light emitting diodes (LEDs), on the other hand, are not limited by low-quality cavities and can operate efficiently without threshold. LEDs, however, have historically been overlooked because their modulation speeds are limited by the relatively slow process of spontaneous emission. Recently, significant progress has been made to increase the rate of spontaneous emission from both dye molecules[9−12] and semiconductor materials[13−19] using optical antennas, opening up the possibility of an efficient, high speed, nanoscale emitter. While several methods have been developed to couple metal-cavity nanolasers to optical waveguides,[20,21] semiconductors to lossy plasmonic[22,23] and dielectric[24] waveguides, and dipole emission into free-space with near unity collection efficiency,[25−27] it has never been demonstrated that an antenna-enhanced nanoLED can be efficiently coupled to a low-loss optical waveguide. This is a crucial step required to enable the use of antenna-enhanced nanoemitters in on-chip links.

In this Letter we demonstrate that the light emitted from an optical antenna-based nanoLED can be efficiently coupled into an integrated InP waveguide using top-down fabrication processes. While traditional LEDs are difficult to efficiently couple to single and few-mode waveguides due to a large spatial mode mismatch, a nanoscale LED that is significantly smaller than the emission wavelength can be spatially coherent, allowing for efficient waveguide coupling.[28,29] By properly engineering the waveguide width and thickness, large coupling efficiencies of 77% can be achieved. Furthermore, by utilizing a directional antenna, the optical version of a Yagi−Uda, coupling efficiencies up to 70% with directional emission are demonstrated while simultaneously allowing the antenna to enhance the rate of spontaneous emission by 36×.

The LED structure used here is based off the arch-antenna design.[19,30] The structure uses an InGaAsP nanoridge 150 nm long, 40 nm wide, and 35 nm tall formed through wet etching as the emitting material. A gold bar is deposited perpendicularly over the ridge which creates a dipole antenna with a metal arch over the ridge acting as an LC tuning network (Figure 1a). This structure has been shown to efficiently enhance the spontaneous emission rate of the InGaAsP emitter, with efficient rate enhancements as large as 2500× possible for a properly scaled down device. In free space, this structure has a dipole-antenna-like donut radiation pattern,[31] which is isotropic in all directions perpendicular to the length of the antenna as

Received: February 10, 2015
Revised: March 30, 2015
Published: April 1, 2015

DOI: 10.1021/acs.nanolett.5b00574
Nano Lett. 2015, 15, 3329−3333

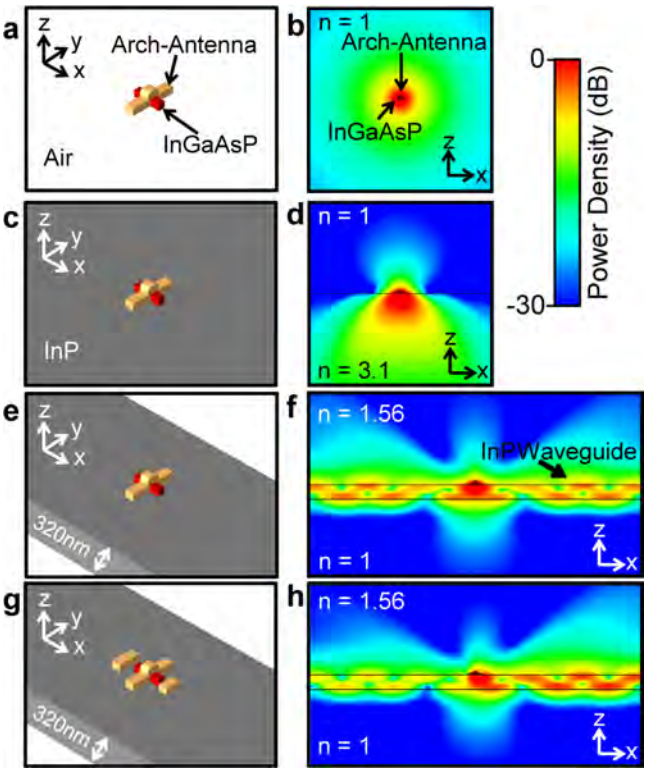

Figure 1. Perspective view and simulated power density emitted from a nanoLED in air (a,b) on an InP Substrate (c,d) on a 320 nm thick waveguide (e,f) and on a waveguide with a passive reflector and director (g,h).

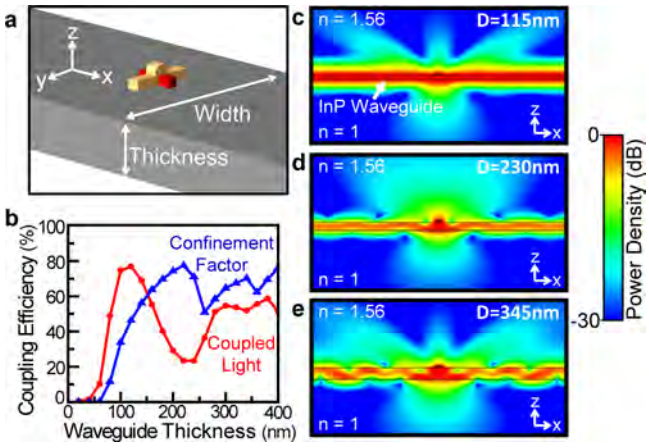

Figure 2. (a) Perspective view of the arch-antenna nanoLED sitting on an InP waveguide. (b) Simulated coupling efficiency (red) and waveguide confinement factor (blue) of light emitted from the nanoLED for waveguides of varying thickness. Power density plot of light emitted from the nanoLED into a (c) 115 nm, (d) 230 nm, and (e) 345 nm thick waveguide.

shown in Figure 1b. With the structure sitting on an InP substrate, the majority of the light is coupled downward into the high-index substrate (Figure 1d). As is well-known in bulk LED's, most of this light will be trapped in the substrate and not be able to radiate into free space.[32] By restricting the thickness and width of the InP substrate, an optical waveguide can be formed which utilizes this concept of light trapping to guide light around a chip.

Figure 2a depicts an arch-antenna sitting on a slab of InP of finite width and thickness to form a waveguide. The waveguide is cladded in $-z$ direction by vacuum (n = 1) and in the $+z$ direction by a medium index material (n = 1.56) similar to oxide or epoxy. To determine the effect of waveguide thickness on antenna emission patterns, time domain simulations (CST Microwave Studio) were performed using a dipole excitation at the center of an InGaAsP ridge 150 nm long, 40 nm wide, and 35 nm tall. The waveguide was made sufficiently long ($\pm$10 μm) so the total power flowing out of the simulation domain in the $\pm x$ direction could be taken as the total power coupled into the waveguide. The waveguide coupling efficiency was then calculated as the ratio of power coupled into the waveguide to the total radiated power, and the confinement factor was calculated as the ratio of power confined within the waveguide to total power coupled into the waveguide mode. With the waveguide width kept at a constant 500 nm, the thickness was varied and the subsequent coupling efficiencies and confinement factors were calculated and are plotted in Figure 2b. All simulation results are for a wavelength of 1300 nm.

Peak coupling efficiency occurs when the waveguide is ~115 nm thick, which is approximately $\lambda/4$. This implies that maximum coupling occurs when light emitted in the $-z$ direction reflects off the bottom interface of the waveguide and destructively interferes with light emitted in the $+z$ direction. This can be seen in Figure 2c where light emitted normal to the waveguide into the $+z$ direction is attenuated and the principle $+z$ emission is at large angles. Oppositely, the minimum coupling efficiency occurs when the waveguide is ~230 nm thick, or approximately $\lambda/2$. This corresponds to when light reflecting off the bottom interface of the waveguide constructively interferes with light emitted in the $+z$ direction. Correspondingly, this can be seen in Figure 2d where there is a strong intensity of light emitted normal to the waveguide in the $+z$ direction. The coupling efficiency peaks again around $3\lambda/4$, ~345 nm, for which its emission pattern shown in Figure 2e is similar to the $\lambda/4$ waveguide, except at this thickness the waveguide is multimode. Further increases to the waveguide thickness have little effect on the coupling efficiency.

The confinement factor, depicted in Figure 2b, monotonically increases with increasing thickness, while the waveguide is single-mode. Once the waveguide becomes multimode at a thickness of ~230 nm, light can couple into a higher order mode which offers lower confinement. As a result, the confinement factor begins to drop. Even though a second mode is available at a thickness of 240 nm, the coupling efficiency remains low due to the destructive interference effect. As the waveguide increases in thickness and more modes are accessible, the relation between confinement factor and coupling efficiency becomes more complicated since many different spatially overlapping modes come into play. Since light is deterministically emitted into a few modes of the waveguide, later mode conversion could be used to combine the coupled light into a single mode. More detailed engineering of the mode structure is an interesting topic that requires further investigation.

The effect of waveguide width on coupling efficiency and confinement factor is investigated in the Supporting Information. Unlike previous work coupling dye molecules and quantum dots to subwavelength cylindrical fibers,[29,33] we find the waveguide width has a minimal impact on coupling, especially compared to the waveguide thickness. This suggests that the effect of constructive and destructive interference plays

DOI: 10.1021/acs.nanolett.5b00574
Nano Lett. 2015, 15, 3329−3333

a larger role in coupling than just squeezing the optical mode into a smaller dimension.

For all further antenna structure simulations and actual device fabrication, a waveguide thickness of 320 nm is chosen. This thickness offers high optical confinement as well as coupling efficiencies up to 70% depending on the width of the waveguide. While a $\lambda/4$ waveguide would offer slightly higher coupling, the higher confinement of the thicker waveguide is advantageous as it will decrease scattering losses as light propagates down the waveguide.

Figure 1f depicts the simulated power density of light emitted from an arch-antenna sitting on an InP waveguide 320 nm thick and 880 nm wide. Due to the symmetry of the structure, an equal amount of light is coupled in both the $+x$ and $-x$ direction along the waveguide. For a point to point optical link, the light would ideally be directed in a single direction down the waveguide. There are two main approaches to realize this: a directional antenna could be used in place of the arch-antenna, or one direction of the waveguide could be truncated with a reflective element such as a dielectric or metal mirror. We will focus on the case of using a directive antenna and briefly touch on the use of a truncated waveguide in the Supporting Information.

Yagi–Uda antenna structures have been shown to be effective in directing optical light in a preferred direction.[34−37] The arch-antenna can be used as the driven element in a Yagi–Uda structure by adding a passive reflector element behind it and a director element in front as depicted in Figure 1g. The simplest element to fabricate is a single gold bar without a feedgap. In order for the light scattered from the reflector and director to have the correct phase shift to constructively interfere in the forward direction, the reflector and director are slightly detuned from resonance. The reflector is made slightly longer than the resonant length, while the director is made slightly shorter than the resonant length.[38] The resonant length of a simple gold bar, however, is not the same as an arch-antenna which has additional reactance from the metal arch over the ridge.[19] Simulations show that a 50 nm wide, 40 nm thick gold bar sitting on InP must be 125 nm long to be resonant at a wavelength of 1300 nm, compared to 250 nm long for an arch-antenna of the same width and thickness. This will cause both the reflector and director elements to be shorter than the driven element. While it is counterintuitive that a small element can efficiently direct emission from a longer driven element, it is well-known that small linear antennas have a scattering cross-section independent of length.[31,38] Therefore, even a short element can affect fields within an area much larger than their physical size.

A parametric simulation sweep of reflector and director lengths and spacings was performed to optimize emission into the $+x$ direction. The minimum element spacing was set by the length of the InGaAsP ridge extending out from the arch-antenna, ∼50 nm depending on alignment tolerances. Simulations find that for a director length (spacing) of 75 nm (105 nm) and a reflector length (spacing) of 135 nm (125 nm), a front to back emission ratio of 3:1 can be achieved with a coupling efficiency of 68%. Figure 1h demonstrates that for a well-tuned Yagi–Uda configuration, the arch-antenna excites the same waveguide mode as the nondirectional case, but now light is preferentially emitted in the $+x$ direction.

To experimentally validate the coupling efficiencies calculated in Figure 2, a nanoLED was fabricated on a 320 nm thick InP epi layer. The InP layer was then patterned into a waveguide 50 μm long with widths varying between 680 nm and 3 μm. The entire structure was bonded to a quartz carrier, and the substrate was completely removed. This allows the waveguide to be measured without any complications of light coupling into the substrate.

Optical emission measurements were performed by optically injecting carriers into the InGaAsP ridge using a Ti:sapphire laser with center wavelength of 720 nm that was focused onto the ridge with a 100× 0.8 NA objective. The laser is polarized perpendicular to the antenna to minimize pump enhancement in the antenna-coupled ridge (see Supporting Information). The InP waveguide is absorbing at the pump wavelength which allows for a greater amount of carriers to be injected into the InGaAsP and also helps minimize the effect of the antenna on pumping conditions. With equivalent pumping and surface recombination conditions, an increase in optical emission is a direct measurement of the increased rate of spontaneous emission into the farfield as detailed in ref 19. A thin 3 nm atomic-layer deposition TiO_2 layer ensures the surface of the InGaAsP is the same for both bare and antenna-coupled ridges.

Light emitted from the structure was either collected with the same objective used to pump the sample or through a second 100× 0.8 NA objective on the opposing side of the pump objective as shown in Figure 3a. By using two identical

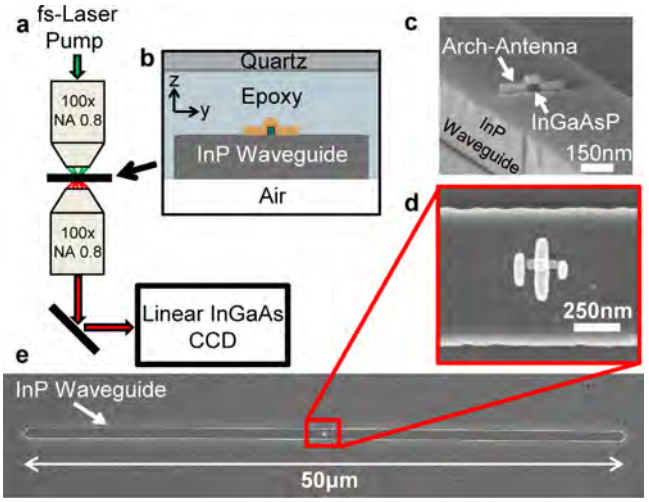

Figure 3. (a) Schematic of measurement setup. (b) Cross section of nanoLED on an InP waveguide bonded to a quartz handle wafer with epoxy. (c) Perspective and (d) top-down SEM of fabricated nanoLED structure on a 320 nm thick InP layer. (e) Top view SEM of fabricated nanoLED on a 50 μm long InP waveguide.

objectives, the pump can be kept constant, and emitted light can be collected from both the top and bottom side of the sample. Collected light was either directly detected with a linear InGaAs CCD to observe the spatial pattern of emitted light or fed through a spectrometer first to determine spectral information.

Light emitted by the InGaAsP ridge is either coupled into the InP waveguide or radiates out into free space. The coupled light will travel down the waveguide, and when it reaches the end facet the majority will scatter out (>70%), while the remainder will be reflected back into the waveguide and bounce back and forth between the two ends until it eventually scatters out. Sidewall roughness can be ignored since even an overly pessimistic propagation loss of 10 dB/cm would only yield 1.1% loss from one end of the waveguide to the other. By

DOI: 10.1021/acs.nanolett.5b00574
Nano Lett. 2015, 15, 3329−3333

imaging the waveguide with the InGaAs CCD, it can be determined from where light is being emitted. Light that is not coupled to the waveguide will come directly from the antenna at the center of the waveguide, while the coupled light will be scattered out the ends of the waveguide.

The spatial image captured by the CCD of light emitted from a 3 μm wide waveguide structure is shown in Figure 4b. At the very center of the waveguide, where the single device is located, there is a large peak corresponding to light that is coming directly from the device without coupling into the waveguide. There is then very little light observed until the end of the waveguide 25 μm from the center, corresponding to light that has been coupled into the waveguide and then scattered out the end. For the bidirectional structures the central peak is the largest since the coupled light is split into two peaks at either side of the waveguide. To estimate the coupling efficiency, the number of photons collected from the two ends of the waveguide is compared to the total number of photons collected. Doing this calculation based on the data in Figure 4b yields coupling efficiencies of 57.5%, 43.9%, and 71.5% for the bare, arch-antenna coupled, and Yagi–Uda coupled cases, respectively. Evaluation of the simulated farfield emission patterns (see Supporting Information) suggests this gives a reasonable estimation of coupling efficiency. Similar devices within the same sample show similar coupling results, with fabrication variability having a larger effect on total light collected.

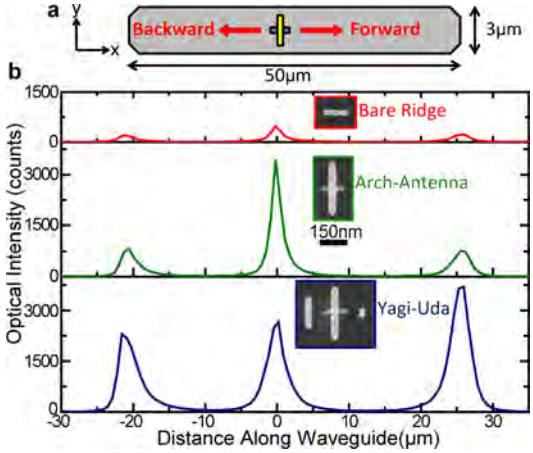

Figure 4. (a) Schematic drawing of waveguide with single device at the center indicating forward and backward directions. (b) Light intensity as a function of distance along the waveguide for a bare ridge (red) 250 nm long arch-antenna (green) and a Yagi–Uda antenna (blue).

Figure 4b also demonstrates enhanced light emission from the arch-antenna. Although the bare ridge and arch-antenna show similar coupling efficiencies, ~5× more light is emitted from the arch-antenna structure with enhancements as large as 12× observed (see Supporting Information). Simulations predict a maximum rate enhancement under the arch of the antenna of 87×. Due to poor diffusion in the nanoridge, only approximately one-third of the carriers in the InGaAsP ever see the antenna (see Supporting Information). This means the 12× increase in light emission for our best devices corresponds to a peak rate enhancement in the antenna feedgap of 36×. Imperfections such as imperfect metal coating of the ridge, size variations in the ridge width (±5 nm), and spatial averaging away from the antenna hotspot under the ridge could account for the remaining discrepancy between simulation and experiment.

The Yagi–Uda structure also shows large enhancement, ~11× more light compared to the bare ridge, but with higher coupling efficiency and directional emission. Yagi–Uda structures on a 3 μm wide waveguide showed front-to-back ratios of ~1.6:1. This figure is limited by reflections at the end facet of the waveguide. Narrower waveguides with tapered end facets show front-to-back ratios as high as 3:1 (see Supporting Information), in good agreement with simulated values.

In summary, we have demonstrated a nanoridge of InGaAsP coupled to an optical antenna with enhanced spontaneous emission into to a low-loss integrated InP waveguide. Experimental results agree well with simulation, demonstrating that with a directional antenna 70% of the emitted light can be effectively coupled into a waveguide. Due to the deep subwavelength size of the optical emitter, light is deterministically emitted into a few modes of the waveguide, which could allow for later mode conversion to a single mode. Alternatively, simulations suggest coupling efficiencies as high as 77% for a single element antenna are possible directly into a single mode waveguide whose thickness has been properly engineered. Such a device offers the possibility of a fast, efficient, nanoscale source for on-chip communication.

■ ASSOCIATED CONTENT

Supporting Information

Details on device fabrications, results from 880 nm wide waveguides, simulated radiation enhancement, the effect of optical pumping on enhanced light emission, a detailed look at the collection efficiencies for optical measurements, comparison between measured and simulated coupling efficiencies, and the effect of waveguide width on coupling efficiency. This material is available free of charge via the Internet at http://pubs.acs.org.

■ AUTHOR INFORMATION

Corresponding Author

*E-mail: wu@eecs.berkeley.edu.

Author Contributions

M.S.E. performed the device simulations, fabricated the devices, designed the experiments, collected the data, and wrote the manuscript. M.C.W. developed the concept and edited the manuscript.

Notes

The authors declare no competing financial interest.

■ ACKNOWLEDGMENTS

National Science Foundation (NSF) Center for Energy Efficient Electronics Science (E3S) award ECCS-0939514; AFOSR award FA9550-09-1-0598.

■ REFERENCES

(1) Lam, C.; Liu, H.; Koley, B.; Zhao, X.; Kamalov, V.; Gill, V. *Commun. Mag. IEEE* **2010**, *48* (7), 32–39.

(2) Miller, D. A. *Proc. IEEE, Spec. Issue Silicon Photonics* **2009**, *97* (7), 1166–1185.

(3) Hill, M. T.; Oei, Y.-S.; Smalbrugge, B.; Zhu, Y.; de Vries, T.; van Veldhoven, P. J.; van Otten, F. W. M.; Eijkemans, T. J.; Turkiewicz, J. P.; de Waardt, H.; Geluk, E. J.; Kwon, S.-H.; Lee, Y.-H.; Nötzel, R.; Smit, M. K. *Nat. Photonics* **2007**, *1* (10), 589–594.

(4) Oulton, R. F.; Sorger, V. J.; Zentgraf, T.; Ma, R.-M.; Gladden, C.; Dai, L.; Bartal, G.; Zhang, X. *Nature* **2009**, *461* (7264), 629–632.

DOI: 10.1021/acs.nanolett.5b00574
Nano Lett. 2015, 15, 3329–3333

(5) Yu, K.; Lakhani, A.; Wu, M. C. *Opt. Express* **2010**, *18* (9), 8790−8799.
(6) Ding, K.; Liu, Z. C.; Yin, L. J.; Hill, M. T.; Marell, M. J. H.; van Veldhoven, P. J.; Nöetzel, R.; Ning, C. Z. *Phys. Rev. B* **2012**, *85* (4), 041301−041305.
(7) Khajavikhan, M.; Simic, A.; Katz, M.; Lee, J. H.; Slutsky, B.; Mizrahi, A.; Lomakin, V.; Fainman, Y. *Nature* **2012**, *482* (7384), 204−207.
(8) Ding, K.; Ning, C. Z. *Semicond. Sci. Technol.* **2013**, *28* (12), 124002.
(9) Kuhn, S.; Mori, G.; Agio, M.; Sandoghdar, V. *Mol. Phys.* **2008**, *106* (7), 893−908.
(10) Kinkhabwala, A.; Yu, Z.; Fan, S.; Avlasevich, Y.; Müllen, K.; Moerner, W. E. *Nat. Photonics* **2009**, *3* (11), 654−657.
(11) Novotny, L.; van Hulst, N. *Nat. Photonics* **2011**, *5* (2), 83−90.
(12) Lee, K.-G.; Eghlidi, H.; Chen, X.-W.; Renn, A.; Götzinger, S.; Sandoghdar, V. *Opt. Express* **2012**, *20* (21), 23331.
(13) Farahani, J. N.; Pohl, D. W.; Eisler, H.-J.; Hecht, B. *Phys. Rev. Lett.* **2005**, *95* (1), 017402.
(14) Fattal, D.; Fiorentino, M.; Tan, M.; Houng, D.; Wang, S. Y.; Beausoleil, R. G. *Appl. Phys. Lett.* **2008**, *93* (24), 243501.
(15) Barth, M.; Schietinger, S.; Fischer, S.; Becker, J.; Nüsse, N.; Aichele, T.; Löchel, B.; Sönnichsen, C.; Benson, O. *Nano Lett.* **2010**, *10* (3), 891−895.
(16) Pfeiffer, M.; Lindfors, K.; Wolpert, C.; Atkinson, P.; Benyoucef, M.; Rastelli, A.; Schmidt, O. G.; Giessen, H.; Lippitz, M. *Nano Lett.* **2010**, *10* (11), 4555−4558.
(17) Arbel, D.; Berkovitch, N.; Nevet, A.; Peer, A.; Cohen, S.; Ritter, D.; Orenstein, M. *Opt. Express* 2011, *19* (10).
(18) Cho, C.-H.; Aspetti, C. O.; Turk, M. E.; Kikkawa, J. M.; Nam, S.-W.; Agarwal, R. *Nat. Mater.* **2011**, *10*, 669−675.
(19) Eggleston, M. S.; Messer, K.; Zhang, L.; Yablonovitch, E.; Wu, M. C. *Proc. Natl. Acad. Sci. U. S. A.* **2015**, 201423294.
(20) Ding, Q.; Mizrahi, A.; Fainman, Y.; Lomakin, V. *Opt. Lett.* **2011**, *36* (10), 1812−1814.
(21) Kim, M.-K.; Lakhani, A. M.; Wu, M. C. *Opt. Express* **2011**, *19* (23), 23504.
(22) Akimov, A. V.; Mukherjee, A.; Yu, C. L.; Chang, D. E.; Zibrov, A. S.; Hemmer, P. R.; Park, H.; Lukin, M. D. *Nature* **2007**, *450* (7168), 402−406.
(23) Huang, K. C. Y.; Seo, M.-K.; Sarmiento, T.; Huo, Y.; Harris, J. S.; Brongersma, M. L. *Nat. Photonics* **2014**, *8* (3), 244−249.
(24) Kolchin, P.; Pholchai, N.; Mikkelsen, M. H.; Oh, J.; Ota, S.; Islam, M. S.; Yin, X.; Zhang, X. *Nano Lett.* **2015**, *15* (1), 464−468.
(25) Esteban, R.; Teperik, T. V.; Greffet, J. J. *Phys. Rev. Lett.* **2010**, *104* (2), 026802.
(26) Lee, K. G.; Chen, X. W.; Eghlidi, H.; Kukura, P.; Lettow, R.; Renn, A.; Sandoghdar, V.; Götzinger, S. *Nat. Photonics* **2011**, *5* (3), 166−169.
(27) Chu, X.-L.; Brenner, T. J. K.; Chen, X.-W.; Ghosh, Y.; Hollingsworth, J. A.; Sandoghdar, V.; Götzinger, S. *Optica* **2014**, *1* (4), 203.
(28) Hwang, J.; Hinds, E. A. *New J. Phys.* **2011**, *13* (8), 085009.
(29) Yalla, R.; Le Kien, F.; Morinaga, M.; Hakuta, K. *Phys. Rev. Lett.* **2012**, *109* (6), 063602.
(30) Seok, T. J.; Jamshidi, A.; Eggleston, M.; Wu, M. C. *Opt. Express* **2013**, *21* (14), 16561−16569.
(31) Sokolnikoff, S. A.; Friis, H. T. *Antennas: Theory and Practice*; John Wiley & Sons, Inc.: New York, 1952.
(32) Schubert, E. F. *Light-Emitting Diodes*, 2nd ed..; Cambridge University Press: Cambridge, U.K., 2006.
(33) Faez, S.; Türschmann, P.; Haakh, H. R.; Götzinger, S.; Sandoghdar, V. *Phys. Rev. Lett.* **2014**, *113* (21), 213601.
(34) Kosako, T.; Kadoya, Y.; Hofmann, H. F. *Nat. Photonics* **2010**, *4* (5), 312−315.
(35) Curto, A. G.; Volpe, G.; Taminiau, T. H.; Kreuzer, M. P.; Quidant, R.; van Hulst, N. F. *Science* **2010**, *329* (5994), 930−933.
(36) Dregely, D.; Taubert, R.; Dorfmüller, J.; Vogelgesang, R.; Kern, K.; Giessen, H. *Nat. Commun.* **2011**, *2*, 267.
(37) Maksymov, I. S.; Staude, I.; Miroshnichenko, A. E.; Kivshar, Y. S. *Nanophotonics* **2012**, *1* (1), 65−81.
(38) Balanis, C. A. *Antenna Theory: Analysis and Design*, 3rd ed.; John Wiley & Sons, Inc.: Hoboken, NJ, 2005.

DOI: 10.1021/acs.nanolett.5b00574
Nano Lett. 2015, 15, 3329−3333